EMBO reports

EMBO open

scientific report

Substrate-induced DNA strand misalignment during catalytic cycling by DNA polymerase λ

Katarzyna Bebenek[1], Miguel Garcia-Diaz[1†]*, Meredith C. Foley[2], Lars C. Pedersen[1], Tamar Schlick[2] & Thomas A. Kunkel[1+]*

[1]Laboratory of Structural Biology and Laboratory of Molecular Genetics, National Institute of Environmental Health Sciences, National Institutes of Health, Research Triangle Park, North Carolina, USA, and [2]Department of Chemistry, Courant Institute of Mathematical Sciences, New York University, New York, New York, USA

The simple deletion of nucleotides is common in many organisms. It can be advantageous when it activates genes beneficial to microbial survival in adverse environments, and deleterious when it mutates genes relevant to survival, cancer or degenerative diseases. The classical idea is that simple deletions arise by strand slippage. A prime opportunity for slippage occurs during DNA synthesis, but it remains unclear how slippage is controlled during a polymerization cycle. Here, we report crystal structures and molecular dynamics simulations of mutant derivatives of DNA polymerase λ bound to a primer–template during strand slippage. Relative to the primer strand, the template strand is in multiple conformations, indicating intermediates on the pathway to deletion mutagenesis. Consistent with these intermediates, the mutant polymerases generate single-base deletions at high rates. The results indicate that dNTP-induced template strand repositioning during conformational rearrangements in the catalytic cycle is crucial to controlling the rate of strand slippage.

Keywords: DNA polymerase; DNA strand slippage; single nucleotide deletions; indels

EMBO reports (2008) **9**, 459–464. doi:10.1038/embor.2008.33

[1]Laboratory of Structural Biology and Laboratory of Molecular Genetics, National Institute of Environmental Health Sciences, NIH, Research Triangle Park, North Carolina 27709, USA
[2]Department of Chemistry, Courant Institute of Mathematical Sciences, New York University, 251 Mercer Street, New York, New York 10012, USA
[†]Present address: Department of Pharmacological Sciences, SUNY at Stony Brook, Stony Brook, New York, USA
*These authors contributed equally to this work
[+]Corresponding author. Tel: +1 919 541 2644; Fax: +1 919 541 7613; E-mail: kunkel@niehs.nih.gov

Received 19 November 2007; revised 22 January 2008; accepted 30 January 2008; published online 28 March 2008

INTRODUCTION

The geometric and kinetic basis by which DNA polymerases prevent the incorporation of incorrect dNTPs, and thereby avoid base substitution errors, has been studied extensively. In comparison, fewer studies have investigated the mechanisms by which simple nucleotide insertion–deletion mutations ('indels') are avoided, such as those occurring at microbial contingency loci (Moxon *et al*, 2006) or those that mutate genes relevant to survival, cancer (Peltomaki, 2003) or degenerative diseases (Pearson *et al*, 2005). For more than 40 years, the main hypothesis to explain indels has been strand slippage in repetitive sequences to generate misaligned DNA that contains extra bases in one strand (Streisinger *et al*, 1966). That strand slippage does occur is evidenced by studies showing that indel mismatches arise during synthesis by all DNA polymerases examined so far, at rates that vary considerably and that can be very high, depending on the DNA polymerase and the sequence context (Kunkel, 2004; Garcia-Diaz & Kunkel, 2006).

The first step in indel formation during DNA synthesis is the strand slippage event itself, which could occur during the synthesis of any DNA sequence. This must be followed by the formation of a stable misaligned intermediate that can be extended by further polymerization. Streisinger's seminal idea was that if slippage was to occur, then slippage in repetitive sequences would allow misaligned intermediates to form that could be stabilized by correct base pairing. Support for Streisinger's idea comes from various observations (for a review, see Garcia-Diaz & Kunkel, 2006) including structural studies showing that DNA polymerase λ (pol λ), an enzyme that is particularly prone to generating single-base deletions during DNA synthesis (Bebenek *et al*, 2003), can bind in a catalytically competent manner to a misaligned primer–template stabilized by correct base pairing and containing an extrahelical base in the template strand upstream of the polymerase active site (Garcia-Diaz & Kunkel, 2006).

The ability of DNA polymerases to bind to and to extend a misaligned intermediate raises the question of how the formation of misalignment is initiated— that is, how and when strand slippage occurs during a polymerization cycle. Several ideas have been proposed (for reviews, see Potapova *et al*, 2002; Johnson *et al*, 2003; Garcia-Diaz & Kunkel, 2006). According to one model (Kunkel, 1986; Hashim *et al*, 1997), slippage might be initiated when an incoming dNTP pairs directly with a base that is adjacent to the normal template base, leaving an uncopied base in the polymerase active site that is eventually deleted or added. Structural analysis of *Sulfolobus solfataricus* (*Sso*) DNA polymerase IV (Dpo4; Ling *et al*, 2001) supports this model, which might be relevant to the subset of DNA polymerases that can simultaneously accommodate two template nucleotides in the binding pocket of the nascent base pair—that is, certain Y polymerases. Another proposal is that slippage might be initiated by dNTP misinsertion followed by primer relocation to allow complementary base pairing with an adjacent template base (Kunkel & Soni, 1988); this misinsertion–primer relocation model is limited to specific sequence contexts. A third idea is melting-misalignment, in which strand misalignments are initiated during the movement of a single-stranded primer between the polymerase and 3′ exonuclease active site of a proofreading-proficient DNA polymerase (Fujii *et al*, 1999). This idea is relevant to the minority of DNA polymerases that have 3′-exonuclease activity.

Although the three initiation ideas mentioned above might be important to a subset of indels, a fourth idea that might be generally relevant to all polymerases and sequence contexts is slippage initiated as a polymerase dissociates or associates with the primer–template DNA (for a review, see Bebenek & Kunkel, 2000). Generality is implied by the fact that all polymerases make and break many non-covalent contacts with the primer–template DNA during catalytic cycling. A crucial step in any normal template-dependent polymerization cycle is correct dNTP binding. This binding event induces conformational changes in both the polymerase and the primer–template DNA, which lead to assembly of an active site with the geometry required for catalysis. Structural studies of the catalytic cycle of wild-type DNA pol λ, a family X DNA repair enzyme (Garcia-Diaz *et al*, 2005a), revealed that dNTP-induced conformational transitions include a 5 Å repositioning of the template strand relative to the primer strand, a shift in the position of a loop between β strands 3 and 4 in the palm subdomain, and movements of a few side chains that form part of the dNTP-binding pocket (supplementary Fig 1A online). Of particular interest is Arg 517, a conserved residue that, before dNTP binding, stacks with the template base that is 5′ of the primer-terminal base pair (supplementary Fig 1B online). On dNTP binding, Arg 517 relocates, thus allowing the templating base to move into position for catalysis. At that point, the side chain of Arg 517 is in a position to form one minor-groove hydrogen bond with the template base in the active site and another with the template base immediately upstream (supplementary Fig 1A online).

The possible relevance of the repositioning of the templating base for the formation of deletion intermediates has been considered in previous studies (Osheroff *et al*, 2000; Johnson *et al*, 2003). These include one study in which we suggested that repositioning of the template strand relative to the primer strand during catalytic cycling by pol λ provides the opportunity for strand slippage (Garcia-Diaz *et al*, 2005b). The interactions of the Arg 517 side chain with template strand bases indicate that Arg 517 might partly control the propensity for slippage. To test this idea and to gain an insight, at the atomic level, into the mechanism of strand slippage in a catalytic cycle, we investigated the structure and single-base deletion error rates of pol λ mutants containing amino-acid replacements for Arg 517 and conducted molecular dynamics simulations of these systems.

RESULTS AND DISCUSSION

First, we replaced Arg 517 with alanine to remove the side-chain interactions seen in crystal structures of wild-type pol λ (supplementary Fig 1 online). Numerous attempts to obtain a crystal structure of a ternary R517A pol λ●gapped DNA●dNTP complex were unsuccessful. However, we succeeded in obtaining a 2.3 Å resolution crystal structure of a binary complex of R517A pol λ bound to a one-nucleotide gap, the physiologically relevant substrate of pol λ. The crystal contained two molecules of R517A pol λ in the asymmetric unit (Table 1), both of which had surprising and informative structures. In molecule A, the major conformation of the template strand, and the position of a loop between β strands 3 and 4 were similar to those seen in the ternary precatalytic complex of wild-type pol λ (Fig 1A)—that is, they were on the pathway to catalysis. This was unexpected, even more so because the two crucial side chains at the active site (other than Arg 517) remained in the 'inactive' conformations expected of a binary complex before dNTP binding (Fig 1A). The density was consistent with a minor population of template strands in the inactive binary complex conformation. In molecule B, the side chains were also in inactive conformations, and two conformations were clearly observed for the template strand: one (coloured magenta in Fig 1B) resembling that seen with wild-type pol λ in the active (ternary complex) conformation, and the other (yellow) resembling that seen with wild-type pol λ in the inactive (binary complex) conformation. These DNA conformations correlated with two different positions of the loop between β strands 3 and 4. Importantly, although significant differences in the template position were observed, in both A and B molecules the primer strands were in the same position. This position overlays with the primer strands in the binary and ternary complexes of the wild-type enzyme, and it is stabilized by the same protein interactions—that is, with Arg 488 and with the HhH motif in the fingers subdomain (Fig 1C). Thus, replacing the side chain of Arg 517 with the methyl group of alanine has no significant effect on the primer strand, but uncouples the conformational transition of the template from that of the enzyme, thereby allowing the template strand to slip towards an active conformation even in the absence of the correct dNTP. Previous molecular dynamics simulations of this R517A mutant also highlighted the special conformational flexibility of the template strand (Foley *et al*, 2006).

Next, we determined the 2.2 Å resolution structure of a ternary complex of pol λ containing a more conservative lysine replacement for Arg 517 (Table 1). Even this conservative replacement altered the structure of both molecules in the asymmetric unit. The template strand was in a similar position as in the wild-type pol λ ternary complex, but the conformations of the three crucial side chains at the active site (other than Arg 517) were intermediate between those seen in the wild-type pol λ binary (inactive) and ternary (active) complexes (Fig 2).

Table 1 | Summary of crystallographic data

Data set	R517A	R517K
Protein Data Bank ID		
Unit cell dimensions (Å) ($a \times b \times c$)	94.24 × 151.88 × 85.64	94.23 × 150.69 × 85.78
Space group	*P*21212	*P*21212
Number of observations	319,116	345,548
Unique reflections	56,848	60,372
R_{sym} (%) (last shell)*	0.11 (0.60)	0.09 (0.41)
$I/\sigma I$ (last shell)	12.00 (2.11)	14.30 (2.35)
Completeness (%) (last shell)	96.8 (91.5)	96.8 (89.6)
Refinement statistics		
Resolution (Å)	2.25	2.20
R_{cryst} (%)†	22.5	20.1
R_{free} (%)§	26.4	23.6
Number of complexes in the asymmetric unit	2	2
Mean *B* value (Å^2)	33.3	28.6
RMS deviation from ideal values		
Bond length (Å)	0.013	0.006
Bond angle (°)	1.2	1.2
Dihedral angle (°)	22.4	21.9
Improper angle (°)	0.9	0.9
Ramachandran statistics		
Residues in		
Favoured regions (%)	96.9	96.8
Disallowed regions (%)	0.6	0

R517A structure: 5,092 protein atoms with 31.00 mean *b* factor; 848 DNA atoms with 41.88 mean *b* factor; 639 water atoms with 38.75 *b* factor; no divalent metals. R517K: 5,092 protein atoms with 26.37 mean *b* factor; 850 DNA atoms with 30.99 mean *b* factor; 838 water atoms with 36.45 *b* factor; 2 divalent metal ions with 15.57 mean *b* factor. Both structures have been deposited in the Protein Data Bank database and have the accession codes 3C5F and 3C5G.
*$R_{sym} = \sum(|I_i - \langle I \rangle|)/\sum(I_i)$, where I_i is the intensity of the *i*th observation and $\langle I \rangle$ is the mean intensity of the reflection.
†$R_{cryst} = \sum||F_o| |F_c||/\sum|F_o|$, calculated from working data set.
§R_{free} is calculated from 5% of data randomly chosen not to be included in refinement.

These differences might relate to the fact that the ε-amino group of the lysine side chain is positioned away from the template, such that it fails to form a hydrogen bond with the template base in the active site, but can form a water-mediated hydrogen bond with the adjacent template base upstream (Fig 2). These results again indicate that the template strand has increased conformational flexibility when normal interactions with Arg 517 are disturbed.

The same idea emerges from molecular dynamics simulations of ternary complexes of R517A and R517K pol λ mutants. These show that the range of template strand flexibility depends on the mutant system being simulated and that the relative degree of flexibility observed in the simulations closely reflects interactions of the mutant residue with the DNA. Compared with the wild type, the R517A mutant shows approximately 2–4 Å greater motion in the DNA template strand towards the binary position (Fig 3A,B, and corresponding RMSD data in supplementary Fig 2A,D online). Similarly, simulations of the R517K mutant—both with and without the catalytic metal—indicate increased conformational flexibility in the template strand. In the R517K simulation without the catalytic ion, the region of the template strand proximal to Arg 517 in the wild type shows considerable movement towards the binary position (Fig 3C; supplementary Fig 2C online). When the catalytic metal is included in the R517K model, the movement of the template strand is less pronounced (Fig 3D; supplementary Fig 2B online) and is observed only during the early stage of simulation. This suggests that the presence of the catalytic ion might help to stabilize the DNA at the active site. This is consistent with the fact that in the ternary R517K crystal structure, where two metals are bound in the active site, movement of the template is not evident. The R517K mutant simulations also suggest that, unlike the arginine side chain, Lys 517 does not adopt a stable conformation and is flexible, interchanging among three main side-chain orientations (supplementary Fig 3 online). As a consequence, most of the interactions of the arginine side chain with the template strand are not observed or steadily maintained in the R517K mutant (supplementary Fig 4 online). However, consistent with the crystal structure, a water-mediated interaction can occur between

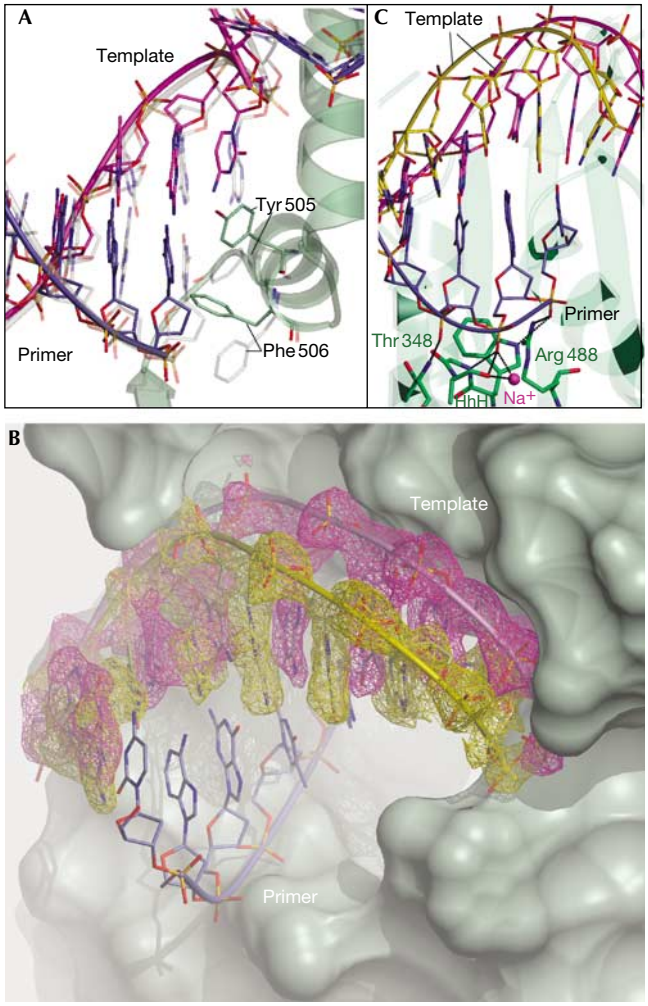

Fig 1 | Crystal structures of the R517A polymerase λ mutant. (**A**) Overlay of molecule A (solid colour; see text) with a polymerase (pol) λ ternary complex (Protein Data Bank entry 1XSN; transparent). In the mutant binary complex, the template strand is located in an analogous conformation to that observed in a wild-type ternary complex, whereas Tyr 505 and Phe 506 are in a binary conformation. (**B**) In molecule B, two conformations are observed for the template strand, corresponding to the binary (yellow) and ternary (magenta) conformations. Two simulated annealing F_o-F_c omit density maps are shown, contoured at 3σ. In one case, the ternary-like conformation was omitted from map calculation (magenta), whereas in the other case the binary-like conformation was omitted (yellow). (**C**) The primer strand in molecule B is maintained in the same conformation by several protein–DNA interactions (see text), whereas the template strand adopts two alternative conformations.

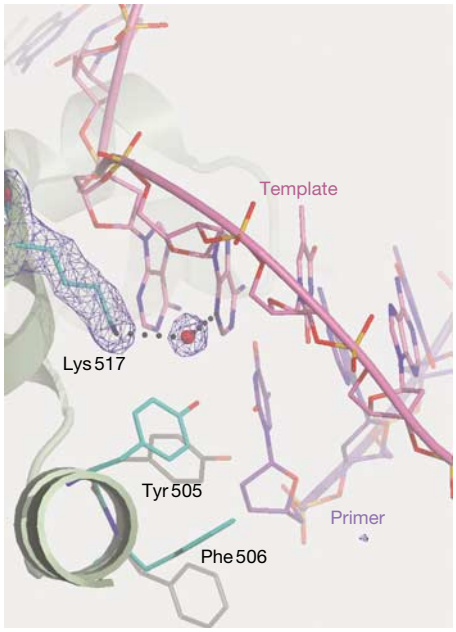

Fig 2 | Crystal structure of R517K polymerase λ. In both molecules in the asymmetric unit, a similar conformation of the Lys 517 side chain (cyan) is observed in a position to establish a water-mediated hydrogen bond with the base of the primer-terminal template nucleotide. A simulated annealing F_o-F_c omit density map is shown in blue, contoured at 6σ. Tyr 505 and Phe 506 are in positions intermediate between those observed in the binary and the ternary structures. The conformation of these side chains in the ternary complex is shown in grey.

Lys 517 and the template base of the primer-terminal base pair (supplementary Table 1 online). In both the R517A and R517K mutant simulations, changes occur to other crucial active-site residues in addition to the mutant residue. Tyr 505 flips to its binary position, as does Phe 506 in one of the R517K simulations, consistent with the intermediate residue conformations observed in the ternary R517K crystal structure. Overall, the results indicate that although the lysine side chain at position 517 provides more template-stabilizing interactions than the alanine side chain, these interactions are still insufficient to ensure template strand stability and an ordered transition to a catalytically active conformation.

The increased conformational flexibility of the template strand conferred by the R517K and R517A replacements predicts that, in comparison with wild-type pol λ, R517A and R517K pol λ might have increased error rates for single-base deletions that involve slipped intermediates with an extra base in the template strand. To test this prediction, we measured the frequency of single-base deletion mutations in a template TTTT during DNA synthesis *in vitro* to fill a 6-nucleotide gap (Bebenek *et al*, 2003). In this assay, wild-type pol λ generated single-base deletions at a frequency of $1.2 \pm 0.25 \times 10^{-2}$. Importantly, the R517K and R517A pol λ mutants had mutation frequencies that were 3.3- and 3.7-fold higher, respectively (Table 2). The lower fidelity of both mutant enzymes correlates with the increased conformational flexibility of the template strand observed in the crystal structures and molecular dynamic simulations. These results indicate that Arg 517 in pol λ is important in coordinating the dNTP-induced repositioning of the template strand during catalytic cycling, in a manner relevant to strand slippage that can result in single-base deletions.

As mentioned in the Introduction, all DNA polymerases make single-base deletions (Tippin *et al*, 2004; Garcia-Diaz & Kunkel, 2006), all polymerases make and break many non-covalent contacts with the primer–template DNA during catalytic cycling

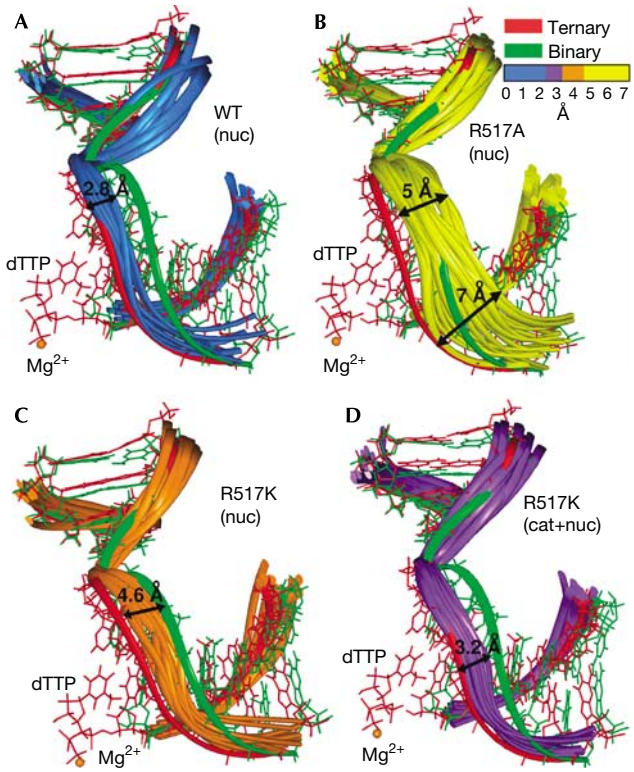

Fig 3 | Range of DNA motion during molecular dynamics simulations of wild-type and mutant (R517A and R517K) polymerase λ systems. The different panels show selected positions of the DNA backbone obtained from simulations of (**A**) wild-type polymerase λ, (**B**) R517A mutant, (**C**) R517K mutant and (**D**) R517K mutant with the catalytic ion. Arrows indicate ranges of DNA motion. The simulated DNA is superimposed on the crystal structures of the binary and ternary complexes (Protein Data Bank (PDB) entry 1XSL, green, and PDB entry 1XSN, red, respectively) to provide a frame of reference. The dTTP and Mg^{2+} from the ternary crystal structure are also shown in each panel. cat, catalytic ion bound; dTTP, 2′-deoxythymidine 5′-triphosphate; Nuc, nucleotide-binding ion bound; WT, wild-type polymerase λ.

and all polymerases assemble their active sites through dNTP-induced conformational changes, including changes in DNA conformation (for reviews, see Goel *et al*, 2002; Johnson *et al*, 2003; Moon, 2007). Thus, dNTP-induced repositioning of the template strand relative to the primer strand during catalytic cycling might provide a general opportunity for indel errors to arise in the context of any of the misalignment models discussed in the Introduction and during various DNA biosynthetic reactions that are catalysed by many different DNA polymerases in cells.

METHODS

Protein and DNA oligonucleotides used for crystallization. The pol λ catalytic core was expressed and purified as described previously (Garcia-Diaz *et al*, 2005b). The following oligonucleotides were used for crystallography: Tb (5′CGGCCGTACTG), Pb (5′CAGTAC), D (5′GCCG); Ttern (5′CGGCAATACTG), Ptern (5′CAGTA).

Protein crystallization and data collection. Mutagenesis was performed by using the Quikchange mutagenesis kit (Stratagene, La Jolla, CA, USA) and the pol λ catalytic core was purified as described previously (Garcia-Diaz *et al*, 2005b). Crystals of the R517A mutant were formed by using the hanging-drop method, by mixing 2 μl of the protein solution containing DNA with 2 μl of reservoir solution containing 0.2 M ammonium acetate, 100 mM Hepes, pH 7, and 10% PEG 4000. Crystals were transferred in five steps to a solution containing 0.2 M ammonium acetate, 100 mM Hepes, pH 7, 12% PEG 4000, 100 mM NaCl, 10 mM $MgCl_2$ and 15% ethylene glycol. Crystals of the R517K protein were formed by using the hanging-drop method, by mixing 2 μl of the protein solution containing DNA with the ddTTP (10 mM) with 2 μl of reservoir solution containing 0.1 M KCl, 10 mM $MgCl_2$, 50 mM Tris–HCl, pH 8.5, and 30% PEG 400. Crystals were transferred in five steps to a solution containing 0.1 M KCl, 10 mM $MgCl_2$, 50 mM Tris–HCl, pH 8.5, 100 mM NaCl and 40% PEG 400. All crystals were frozen in liquid nitrogen and then mounted on a goniometer in a cold stream of nitrogen at −178 °C for data collection. Data were collected on a Rigaku 007HF generator equipped with Varimax HF mirrors and a Saturn 92 detector. All data were processed by using the HKL2000 software (Otwinowski & Minor, 1997). The atomic coordinates and structure factors have been deposited in the Protein Data Bank (PDB) database and have the accession codes 3C5F and 3C5G.

Molecular replacement and refinement. Phases were calculated by using molecular replacement from PDB entries 1XSP or 1XSN as the starting models. The programs O (Jones *et al*, 1991) and Coot (Emsley & Cowtan, 2004) were used for model building and the models were refined with CNS (Brünger *et al*, 1998). In all cases, the density was of sufficient quality to build most side chains and most backbone atoms, with the exception of a few amino-terminal residues and a few residues in disordered loops. The quality of the models was assessed with Molprobity (Lovell *et al*, 2003) and all were found to have good stereochemistry (see Table 1). Figures were made by using Molscript (Kraulis, 1991), Povscript+ (Fenn *et al*, 2003) and POV-Ray (www.povray.org).

Molecular dynamics simulations. Initial energy minimizations and equilibration simulations were performed by using CHARMM (Brooks *et al*, 1983). Production dynamics were performed at constant temperature and volume by using NAMD (Phillips *et al*, 2005) with the CHARMM force field (MacKerell & Banaval,

Table 2 | Single-nucleotide deletion fidelity of wild-type, R517K and R517A polymerase λ

Pol λ	Reversion frequency ($\times 10^{-2}$)
Wild type	1.2 (±0.25)
R517K	4.0 (±0.41)
R517A	4.4 (±0.83)

Pol λ, polymerase λ.
The assay used for measuring the fidelity of the 39 kDa form of pol λ has been described previously (Bebenek *et al*, 2003). DNA synthesis by pol λ was conducted in reaction mixtures (20 μl) containing 50 mM Tris pH 7.5, 2.5 mM $MgCl_2$, 1 mM dithiothreitol, 2 μg of bovine serum albumin, 4% glycerol, 0.5 nM gapped DNA, 50 μM each of dATP, dGTP, dCTP and dTTP, 1 mM ATP, 400 U T4 DNA ligase, and 150, 300 or 500 nM of the 39 kDa domain of wild-type, R517K or R517A pol λ, respectively. After 1 h incubation at 37 °C, reactions were terminated by adding 15 mM EDTA. DNA products were resolved on a 0.8% agarose gel. The copied DNA products were scored for DNA synthesis errors as described previously (Bebenek *et al*, 2003). The *lacZ* reversion frequencies are the average of three or four determinations, with standard deviations shown in parentheses.

2000). Simulations are described in detail in the supplementary information online.

Supplementary information is available at *EMBO reports* online (http://www.emboreports.org).

ACKNOWLEDGEMENTS

We thank Dr B. Beard and Dr T. Darden for critical review of the manuscript. This research was supported by the Intramural Research Program of the National Institutes of Health (NIH), National Institute of Environmental Health Sciences. M.C.F. and T.S. acknowledge research support in part by Philip Morris USA Inc. and Philip Morris International, National Science Foundation grant MCB-0316771, NIH grant R01 ES012692 and the American Chemical Society's Petroleum Research Fund award (PRF #39115-AC4) to T.S. The computations are made possible by support for the SGI Altix 3700 by the National Center for Supercomputing Applications under grant MCA99S021 and by the New York University Chemistry Department resources under grant CHE-0420870.

CONFLICT OF INTEREST

The authors declare that they have no conflict of interest.

REFERENCES

Bebenek K, Kunkel TA (2000) Streisinger revisited: DNA synthesis errors mediated by substrate misalignments. *Cold Spring Harb Symp Quant Biol* **65:** 81–91

Bebenek K, Garcia-Diaz M, Blanco L, Kunkel TA (2003) The frameshift infidelity of human DNA polymerase λ. Implications for function. *J Biol Chem* **278:** 34685–34690

Brooks BR, Bruccoleri RE, Olafson BD, States DJ, Swaminathan S, Karplus M (1983) Charmm: a program for macromolecular energy, minimization, and dynamics calculations. *J Comput Chem* **4:** 187–217

Brünger AT *et al* (1998) Crystallography & NMR system: a new software suite for macromolecular structure determination. *Acta Crystallogr D* **54:** 905–921

Emsley P, Cowtan K (2004) Coot: model-building tools for molecular graphics. *Acta Crystallogr D* **60:** 2126–2132

Fenn TD, Ringe D, Petsko GA (2003) POVScript+: a program for model and data visualization using persistence of vision ray-tracing. *J Appl Crystallogr* **36:** 944–947

Foley MC, Arora K, Schlick T (2006) Sequential side-chain residue motions transform the binary into the ternary state of DNA polymerase λ. *Biophys J* **91:** 3182–3195

Fujii S *et al* (1999) DNA replication errors produced by the replicative apparatus of *Escherichia coli*. *J Mol Biol* **289:** 835–850

Garcia-Diaz M, Kunkel TA (2006) Mechanism of a genetic glissando: structural biology of indel mutations. *Trends Biochem Sci* **31:** 206–214

Garcia-Diaz M, Bebenek K, Gao G, Pedersen LC, London RE, Kunkel TA (2005a) Structure–function studies of DNA polymerase λ. *DNA Repair* **4:** 1358–1367

Garcia-Diaz M, Bebenek K, Krahn JM, Kunkel TA, Pedersen LC (2005b) A closed conformation for the Pol λ catalytic cycle. *Nat Struct Mol Biol* **12:** 97–98

Goel A, Ellenberger T, Frank-Kamenetskii MD, Herschbach D (2002) Unifying themes in DNA replication: reconciling single molecule kinetic studies with structural data on DNA polymerases. *J Biomol Struct Dyn* **19:** 571–584

Hashim MF, Schnetz-Boutaud N, Marnett LJ (1997) Replication of template–primers containing propanodeoxyguanosine by DNA polymerase β. Induction of base pair substitution and frameshift mutations by template slippage and deoxynucleoside triphosphate stabilization. *J Biol Chem* **272:** 20205–20212

Johnson SJ, Taylor JS, Beese LS (2003) Processive DNA synthesis observed in a polymerase crystal suggests a mechanism for the prevention of frameshift mutations. *Proc Natl Acad Sci USA* **100:** 3895–3900

Jones TA, Zou JY, Cowan SW, Kjeldgaard M (1991) Improved methods for building protein models in electron density maps and the location of errors in these models. *Acta Crystallogr A* **47:** 110–119

Kraulis P (1991) MOLSCRIPT: a program to produce both detailed and schematic plots of proteins. *J Appl Crystallogr* **24:** 946–950

Kunkel TA (1986) Frameshift mutagenesis by eucaryotic DNA polymerases *in vitro*. *J Biol Chem* **261:** 13581–13587

Kunkel TA (2004) DNA replication fidelity. *J Biol Chem* **279:** 16895–16898

Kunkel TA, Soni A (1988) Mutagenesis by transient misalignment. *J Biol Chem* **263:** 14784–14789

Ling H, Boudsocq F, Woodgate R, Yang W (2001) Crystal structure of a Y-family DNA polymerase in action: a mechanism for error-prone and lesion-bypass replication. *Cell* **107:** 91–102

Lovell SC, Davis IW, Arendall WB III, de Bakker PI, Word JM, Prisant MG, Richardson JS, Richardson DC (2003) Structure validation by Cα geometry: ϕ, ψ and Cβ deviation. *Proteins* **50:** 437–450

MacKerell ADJ, Banaval NK (2000) All-atom empirical force field for nucleic acids: II. Application to molecular dynamics simulations of DNA and RNA in solution. *J Comput Chem* **21:** 105–120

Moon AF (2007) The X family portrait: structural insights into biological functions of X family polymerase. *DNA Repair* **6:** 1709–1725

Moxon R, Bayliss C, Hood D (2006) Bacterial contingency loci: the role of simple sequence DNA repeats in bacterial adaptation. *Annu Rev Genet* **40:** 307–333

Osheroff WP, Beard WA, Yin S, Wilson SH, Kunkel TA (2000) Minor groove interactions at the DNA polymerase β active site modulate single-base deletion error rates. *J Biol Chem* **275:** 28033–28038

Otwinowski Z, Minor V (1997) Processing of X-ray diffraction data collected in oscillation mode. *Methods Enzymol* **276:** 307–326

Pearson CE, Nichol Edamura K, Cleary JD (2005) Repeat instability: mechanisms of dynamic mutations. *Nat Rev Genet* **6:** 729–742

Peltomaki P (2003) Role of DNA mismatch repair defects in the pathogenesis of human cancer. *J Clin Oncol* **21:** 1174–1179

Phillips JC, Braun R, Wang W, Gumbart J, Tajkhorshid E, Villa E, Chipot C, Skeel RD, Kale L, Schulten K (2005) Scalable molecular dynamics with NAMD. *J Comput Chem* **26:** 1781–1802

Potapova O, Grindley ND, Joyce CM (2002) The mutational specificity of the Dbh lesion bypass polymerase and its implications. *J Biol Chem* **277:** 28157–28166

Streisinger G, Okada Y, Emrich J, Newton J, Tsugita A, Terzaghi E, Inouye M (1966) Frameshift mutations and the genetic code. *Cold Spring Harb Symp Quant Biol* **31:** 77–84

Tippin B, Kobayashi S, Bertram JG, Goodman MF (2004) To slip or skip, visualizing frameshift mutation dynamics for error-prone DNA polymerases. *J Biol Chem* **279:** 45360–45368